Observation of chi(bJ)(1P, 2P) decays to light hadrons

D. M. Asner, K. W. Edwards, J. Reed, R. A. Briere, G. Tatishvili, H. Vogel, P. U. E. Onyisi, J. L. Rosner, J. P. Alexander, D. G. Cassel, J. E. Duboscq, R. Ehrlich, L. Fields, R. S. Galik, L. Gibbons, R. Gray, S. W. Gray, D. L. Hartill, B. K. Heltsley, D. Hertz, J. M. Hunt, J. Kandaswamy, D. L. Kreinick, V. E. Kuznetsov, J. Ledoux, H. Mahlke-Kruger, D. Mohapatra, J. R. Patterson, D. Peterson, D. Riley, A. Ryd, A. J. Sadoff, X. Shi, S. Stroiney, W. M. Sun, T. Wilksen, S. B. Athar, J. Yelton, P. Rubin, B. I. Eisenstein, I. Karliner, S. Mehrabyan, N. Lowrey, M. Selen, E. J. White, J. Wiss, R. E. Mitchell, M. R. Shepherd, D. Besson, T. K. Pedlar, D. Cronin-Hennessy, K. Y. Gao, J. Hietala, Y. Kubota, T. Klein, B. W. Lang, R. Poling, A. W. Scott, P. Zweber, S. Dobbs, Z. Metreveli, K. K. Seth, B. J. Y. Tan, A. Tomaradze, J. Libby, L. Martin, A. Powell, G. Wilkinson, K. M. Ecklund, W. Love, V. Savinov, H. Mendez, J. Y. Ge, D. H. Miller, I. P. J. Shipsey, B. Xin, G. S. Adams, D. Hu, B. Moziak, J. Napolitano, Q. He, J. Insler, H. Muramatsu, C. S. Park, E. H. Thorndike, F. Yang, M. Artuso, S. Blusk, S. Khalil, J. Li, R. Mountain, K. Randrianarivony, N. Sultana, T. Skwarnicki, S. Stone, J. C. Wang, L. M. Zhang, G. Bonvicini, D. Cinabro, M. Dubrovin, A. Lincoln, P. Naik, and J. Rademacker

PHYSICAL REVIEW D **78,** 091103(R) (2008)

Observation of $\chi_{bJ}(1P, 2P)$ decays to light hadrons

D. M. Asner,[1] K. W. Edwards,[1] J. Reed,[1] R. A. Briere,[2] G. Tatishvili,[2] H. Vogel,[2] P. U. E. Onyisi,[3] J. L. Rosner,[3] J. P. Alexander,[4] D. G. Cassel,[4] J. E. Duboscq,[4,*] R. Ehrlich,[4] L. Fields,[4] R. S. Galik,[4] L. Gibbons,[4] R. Gray,[4] S. W. Gray,[4] D. L. Hartill,[4] B. K. Heltsley,[4] D. Hertz,[4] J. M. Hunt,[4] J. Kandaswamy,[4] D. L. Kreinick,[4] V. E. Kuznetsov,[4] J. Ledoux,[4] H. Mahlke-Krüger,[4] D. Mohapatra,[4] J. R. Patterson,[4] D. Peterson,[4] D. Riley,[4] A. Ryd,[4] A. J. Sadoff,[4] X. Shi,[4] S. Stroiney,[4] W. M. Sun,[4] T. Wilksen,[4] S. B. Athar,[5] J. Yelton,[5] P. Rubin,[6] B. I. Eisenstein,[7] I. Karliner,[7] S. Mehrabyan,[7] N. Lowrey,[7] M. Selen,[7] E. J. White,[7] J. Wiss,[7] R. E. Mitchell,[8] M. R. Shepherd,[8] D. Besson,[9] T. K. Pedlar,[10] D. Cronin-Hennessy,[11] K. Y. Gao,[11] J. Hietala,[11] Y. Kubota,[11] T. Klein,[11] B. W. Lang,[11] R. Poling,[11] A. W. Scott,[11] P. Zweber,[11] S. Dobbs,[12] Z. Metreveli,[12] K. K. Seth,[12] B. J. Y. Tan,[12] A. Tomaradze,[12] J. Libby,[13] L. Martin,[13] A. Powell,[13] G. Wilkinson,[13] K. M. Ecklund,[14] W. Love,[15] V. Savinov,[15] H. Mendez,[16] J. Y. Ge,[17] D. H. Miller,[17] I. P. J. Shipsey,[17] B. Xin,[17] G. S. Adams,[18] D. Hu,[18] B. Moziak,[18] J. Napolitano,[18] Q. He,[19] J. Insler,[19] H. Muramatsu,[19] C. S. Park,[19] E. H. Thorndike,[19] F. Yang,[19] M. Artuso,[20] S. Blusk,[20] S. Khalil,[20] J. Li,[20] R. Mountain,[20] K. Randrianarivony,[20] N. Sultana,[20] T. Skwarnicki,[20] S. Stone,[20] J. C. Wang,[20] L. M. Zhang,[20] G. Bonvicini,[21] D. Cinabro,[21] M. Dubrovin,[21] A. Lincoln,[21] P. Naik,[22] and J. Rademacker[22]

(CLEO Collaboration)

[1]*Carleton University, Ottawa, Ontario, Canada K1S 5B6*
[2]*Carnegie Mellon University, Pittsburgh, Pennsylvania 15213, USA*
[3]*Enrico Fermi Institute, University of Chicago, Chicago, Illinois 60637, USA*
[4]*Cornell University, Ithaca, New York 14853, USA*
[5]*University of Florida, Gainesville, Florida 32611, USA*
[6]*George Mason University, Fairfax, Virginia 22030, USA*
[7]*University of Illinois, Urbana-Champaign, Illinois 61801, USA*
[8]*Indiana University, Bloomington, Indiana 47405, USA*
[9]*University of Kansas, Lawrence, Kansas 66045, USA*
[10]*Luther College, Decorah, Iowa 52101, USA*
[11]*University of Minnesota, Minneapolis, Minnesota 55455, USA*
[12]*Northwestern University, Evanston, Illinois 60208, USA*
[13]*University of Oxford, Oxford OX1 3RH, United Kingdom*
[14]*State University of New York at Buffalo, Buffalo, New York 14260, USA*
[15]*University of Pittsburgh, Pittsburgh, Pennsylvania 15260, USA*
[16]*University of Puerto Rico, Mayaguez, Puerto Rico 00681*
[17]*Purdue University, West Lafayette, Indiana 47907, USA*
[18]*Rensselaer Polytechnic Institute, Troy, New York 12180, USA*
[19]*University of Rochester, Rochester, New York 14627, USA*
[20]*Syracuse University, Syracuse, New York 13244, USA*
[21]*Wayne State University, Detroit, Michigan 48202, USA*
[22]*University of Bristol, Bristol BS8 1TL, United Kingdom*

(Received 7 August 2008; published 13 November 2008)

Analyzing $\Upsilon(nS)$ decays acquired with the CLEO detector operating at the CESR e^+e^- collider, we measure for the first time the product branching fractions $\mathcal{B}[\Upsilon(nS) \to \gamma\chi_{bJ}((n-1)P)]\mathcal{B}[\chi_{bJ}(n-1)P) \to X_i]$ for $n = 2$ and 3, where X_i denotes, for each i, one of the 14 exclusive light-hadron final states for which we observe significant signals in both $\chi_{bJ}(1P)$ and $\chi_{bJ}(2P)$ decays. We also determine upper limits for the electric dipole (E1) transitions $\Upsilon(3S) \to \gamma\chi_{bJ}(1P)$.

DOI: 10.1103/PhysRevD.78.091103 PACS numbers: 14.40.Gx, 13.25.Gv

In the 31 years since the first observation of bottomonium, we have learned a great deal about decays of the $\Upsilon(1S, 2S, 3S)$ resonances and transitions among them. Less is known about P-wave states because they are not produced directly in e^+e^- collisions. The spin-triplet χ_b mesons are produced copiously in electric dipole (E1) transitions [1], permitting the recent first observations of inclusive decays of $\chi_{bJ}(nP)$ to $p(\bar{p})$ [2] and to open charm [3]. Nothing else is known about $\chi_{bJ}(nP)$ decays to non-$b\bar{b}$ states. Such processes are of interest as clues in searching

*Deceased.

for states of mass $\sim 10\ \mathrm{GeV}/c^2$, such as $h_b(^1P_1)$ and hybrids, via their exclusive decays.

In this article we report the first observations of decays of $\chi_{bJ}(1P)$ and $\chi_{bJ}(2P)$ into specific final states of light hadrons, where the $\chi_{bJ}(nP)$ states are produced via $\Upsilon(2S) \to \gamma\chi_{bJ}(1P)$ and $\Upsilon(3S) \to \gamma\chi_{bJ}(2P)$. We also determine upper limits on rates for the suppressed E1 transitions $\Upsilon(3S) \to \gamma\chi_{bJ}(1P)$.

We use the same $\Upsilon(nS)$ on-resonance data as in the analysis of Ref. [4], corresponding to $\mathrm{N}_{\Upsilon(nS)} = (20.82 \pm 0.37, 9.32 \pm 0.14, 5.88 \pm 0.10) \times 10^6$ resonance decays for $n = 1$, 2, and 3, respectively, collected by the CLEO III detector [5] at the Cornell Electron Storage Ring. Hadronic events are selected based on the criteria used in the analysis of Ref. [4].

Our signal events have the form $\Upsilon(nS) \to \gamma X_i$, where X_i denotes a specific fully reconstructed final state. We allow a large variety of possibilities for X_i, but to keep the list finite and realistic we impose the following requirements. Each X_i consists of a combination of 12 or fewer "particles," where a "particle" is defined here to be a photon or a charged pion ($\pi^\pm$), kaon ($K^\pm$), or proton ($p/\bar{p}$). Each state X_i must have at least four charged "particles" and conserve overall charge, strangeness, and baryon number. We only consider modes in which photons other than that from the transition are paired into either π^0 or η candidates, of which we only permit four or fewer. Neutral kaon decays into $\pi^+\pi^-$ are also considered. With these criteria, there are 659 separate final states, which act as the basis for our search.

Photon candidates are taken from calorimeter showers that do not match the projected trajectory of any charged particle and which have a lateral shower profile consistent with that of an isolated electromagnetic shower. Each candidate for a $\pi^\pm$, $K^\pm$, and $p/\bar{p}$ must be positively identified as such by a combination of its specific ionization dE/dx, within 3σ, where σ refers to uncertainty due to measurement errors, and, when available, the response of a ring imaging Cherenkov system as in the analysis of Ref. [3]. Candidates for π^0 and η decays to two photons are allowed only if the photon pair mass is within 3σ of the nominal π^0 or η mass. $K^0_S \to \pi^+\pi^-$ candidates, consisting of a pair of vertex-constrained oppositely charged tracks, are required to have effective mass within 3σ of the nominal mass [1] and to have a flight path before decay exceeding twice the longitudinal vertex resolution, whose typical standard deviation is about 1 mm from the e^+e^- interaction point.

We improve sample purity by constraining the transition photon plus the decay products of X_i to the initial $\Upsilon(nS)$ four-momentum with a 4C kinematic fit and requiring the fitted $\chi^2(4C)/\mathrm{dof} < 5$ as in Ref. [6]. The kinematic fit also allows us to improve the resolution on the invariant mass of the X_i by using fitted, instead of measured, four-momenta: we denote this mass by M_{inv}.

Figure 1 shows fits to the M_{inv} distribution of the sum of all 659 modes in (a) $\Upsilon(2S)$ and (b) $\Upsilon(3S)$ data. The natural $\chi_{bJ}(nP)$ widths [7] are expected to be much smaller than the resolution (~ 5 MeV) of the transition photon, which has a mostly Gaussian line shape and a low-energy tail induced by energy leakage out of the crystals used in the algorithm. This *crystal ball* line (CBL) shape is discussed in more detail in Ref. [8]. To fit the M_{inv} distribution in Fig. 1, we use a "reversed" CBL shape with the asymmetric tail on the high side instead of the low side of the peak. The fitted masses of $\chi_{bJ}(1P)$ and $\chi_{bJ}(2P)$ are consistent with the known masses [1]. For background shapes, we use M_{inv} spectra obtained with the same analysis procedure but based on $\Upsilon(1S)$ data, *shifted* by differences in center-of-mass energy while floating normalizations. This procedure appears to represent backgrounds reasonably. Using low-order polynomials instead of $\Upsilon(1S)$ data to represent backgrounds, we obtain consistent results.

With signal shapes, including central values, fixed by a fit to the sum of the 659 modes, we fit the unconstrained photon energy spectra for *each* mode with CBL shapes. We use unconstrained photon energy spectra because calorimeter resolutions are independent of the final states in $\chi_{bJ}(1P, 2P)$ decays. We then determine significances from the fit to each mode as $\sqrt{-2\ln(\mathcal{L}_{wo}/\mathcal{L}_w)}$, where $\mathcal{L}_{wo}$ and $\mathcal{L}_w$ are likelihoods from fits without and with an allowance for signal. We determine the significance from simulta-

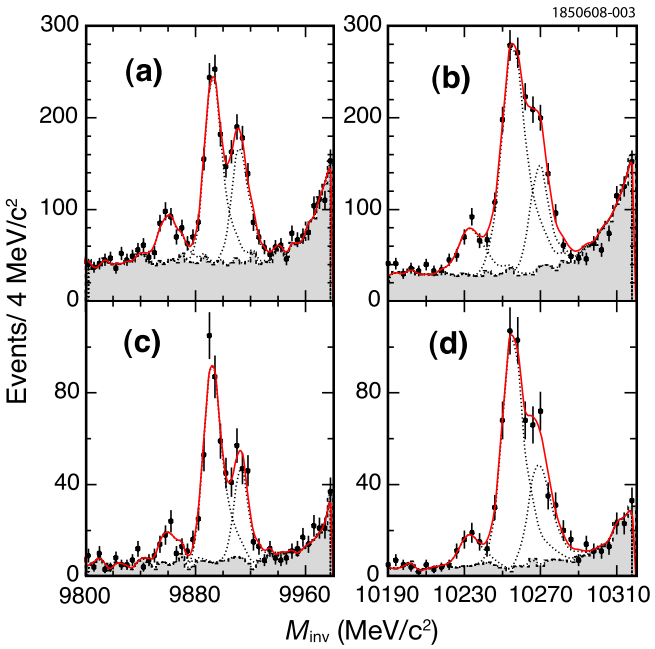

FIG. 1 (color online). M_{inv} spectra based on (a), (c) $\Upsilon(2S)$ and (b), (d) $\Upsilon(3S)$ data for the sum of all 659 modes (a), (b) and the 14 selected modes (c), (d). The observed peaks are consistent with the transitions $\Upsilon(2S) \to \gamma\chi_{bJ}(1P)$ and $\Upsilon(3S) \to \gamma\chi_{bJ}(2P)$. Fitted backgrounds are represented by dashed histograms, fitted $\chi_{bJ}(nP)$ peaks are represented by dotted lines, and sums of fitted signals and background are denoted by solid curves.

neous fits to the three peaks instead of determining the significance of individual $\chi_{bJ}(1P, 2P)$ peaks. We identify 14 modes giving at least 5σ significance from *both* $\chi_{bJ}(1P)$ and $\chi_{bJ}(2P)$ decays.

On the basis of GEANT-based [9] signal and various background Monte Carlo (MC) samples for the 14 identified modes, the required limit on $\chi^2(4C)/\mathrm{dof}$ is varied from its initial value of 5 in order to optimize signal sensitivity while reducing backgrounds. The optimum value for the 14 modes is found to be $\chi^2(4C)/\mathrm{dof} < 3$, and is adopted as our nominal value. As some modes show further improvement in sensitivity for $\chi^2(4C)/\mathrm{dof} < 2$, we also explore the choices $\chi^2(4C)/\mathrm{dof} < 2$ and <4 in our study of systematic uncertainties.

Figure 1 shows M_{inv} distributions of (c) $\Upsilon(2S)$ and (d) $\Upsilon(3S)$ data based on the sum of the 14 modes with our nominal selection criteria. The fitted backgrounds are $\Upsilon(1S)$ data, shifted as in Figs. 1(a) and 1(b). The fitted $\chi_{bJ}(nP)$ masses again are consistent with the known values [1]. With the restriction of $\chi^2(4C)/\mathrm{dof} < 3$, $\Upsilon(2S, 3S)$ decays in the 14 modes lead to roughly 40% of the total observed events in the 659 modes.

To measure $\mathcal{B}[\Upsilon(nS) \to \gamma\chi_{bJ}((n-1)P)]\mathcal{B}[\chi_{bJ}((n-1)P) \to X_i]$, where X_i is each of the 14 modes, fits to signal Monte Carlo samples for signals produced through transitions of $\Upsilon(nS) \to \gamma\chi_{bJ}((n-1)P)$ are performed to M_{inv} spectra. Once signal shapes are fixed for each mode, we perform fits to data. We fix the central values of $\chi_b(1P, 2P)$ masses according to world averages [1]. Fitted $\chi^2(4C)/\mathrm{dof}$ distributions for each mode of $\chi_b(1P, 2P)$ and each J are found to behave as expected from signal MC samples. Resultant fits to M_{inv} spectra are shown in Fig. 2. For all cases, we use a constant (flat) background shape and fitting ranges of 9800–9950 MeV/c^2 in $\Upsilon(2S)$ data and 10180–10300 MeV/c^2 in $\Upsilon(3S)$ data.

The major source of systematic uncertainty is found to be the effects on signal efficiency of possible intermediate states. We study this in $\Upsilon(2S) \to \gamma\chi_b(1P)$ and apply the result to $\Upsilon(3S) \to \gamma\chi_b(2P)$ as well. In all our signal Monte Carlo samples, χ_b decays were generated according to phase space. To estimate the systematic uncertainty due to the presence of intermediate states, we consider $\rho^{\pm} \to \pi^{\pm}\pi^0$, $\rho^0 \to \pi^+\pi^-$, $\phi \to K^+K^-$, $\omega \to \pi^+\pi^-\pi^0$, $\eta \to \pi^+\pi^-\pi^0$, $K^*(892)^0 \to K^{\pm}\pi^{\mp}/K^0_S\pi^0$, and $K^*(892)^{\pm} \to K^{\pm}\pi^0/K^0_S\pi^{\pm}$. We find deviations in the efficiencies based on these modes to be as large as 18%; hence to allow for possible neglected intermediate states, we assign $\pm 20\%$ systematic uncertainty due to MC modeling of $\chi_b(nP)$ decays.

Other sources of systematic errors were found to be small in comparison with the possible presence of intermediate states. In roughly descending order of importance, they are: kinematic fitting (7%–14%); photon, π^0, and charged track reconstruction (4%–10%); particle identification and K^0_S efficiencies (4%–10%); statistical uncertainty on signal MC samples (2%–8%); numbers of $\Upsilon(nS)$ (2%); cross feeds among our 14 signal modes (1%); fit ranges; background shapes; bin width; signal widths; peak positions of χ_b; trigger simulation; and multiple candidates. Systematic errors are added in quadrature mode by mode. They fall within a range of 23%–30% for all modes.

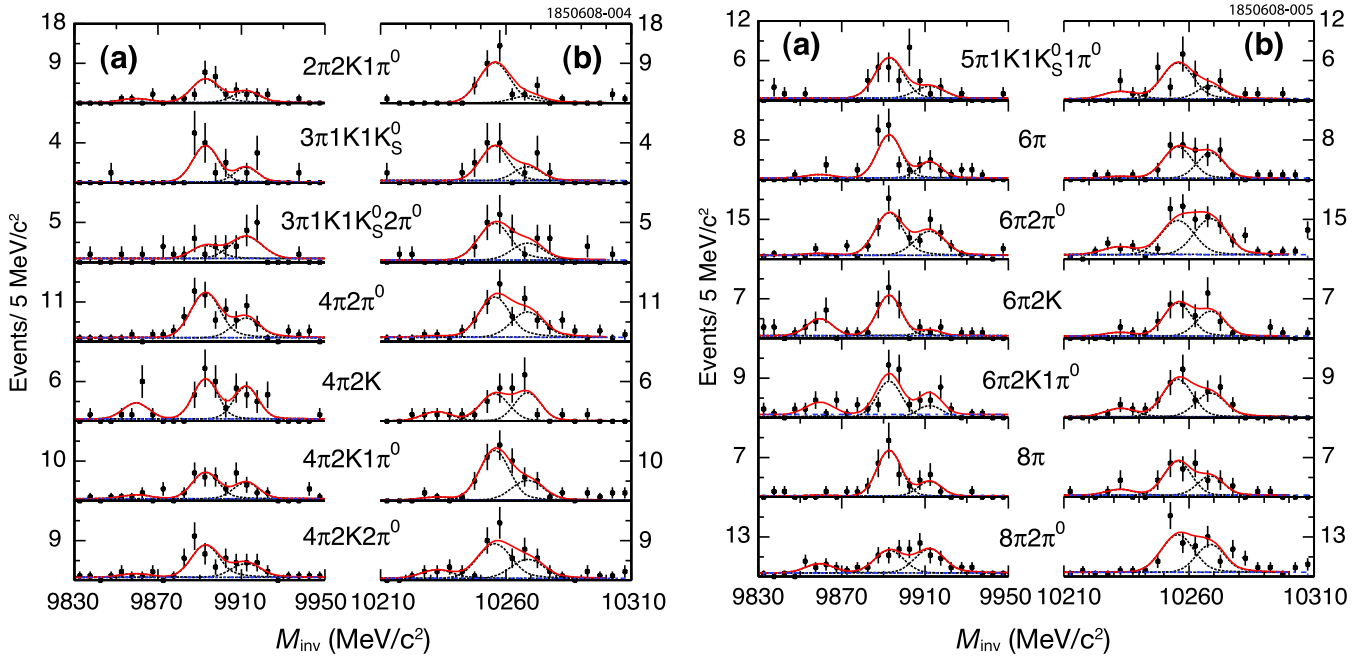

FIG. 2 (color online). Fits to invariant masses of individual decay modes. For each mode X, (a) refers to $\Upsilon(2S) \to \gamma\chi_b(1P)$, $\chi_b(1P) \to X_i$, while (b) refers to $\Upsilon(3S) \to \gamma\chi_b(2P)$, $\chi_b(2P) \to X_i$. Dotted lines represent fitted constant backgrounds while dashed lines are fitted $\chi_{bJ}(nP)$ signals of each J state.

TABLE I. Reconstruction efficiencies for $\Upsilon(nS) \to \gamma + \chi_{bJ}((n-1)P) \to \gamma + X$ (ϵ in units of 10^{-2}), event yields (N) (rounded to the nearest integer), and signal significances (σ) for each of the transitions for each of the 14 modes. In this and subsequent tables $\pi \equiv \pi^{\pm}$, $K \equiv K^{\pm}$.

	$\Upsilon(2S) \to \gamma\chi_{bJ}(1P), \chi_{bJ}(1P) \to X_i$									$\Upsilon(3S) \to \gamma\chi_{bJ}(2P), \chi_{bJ}(2P) \to X_i$								
X_i	$J=0$			$J=1$			$J=2$			$J=0$			$J=1$			$J=2$		
	ϵ	N	σ	ϵ	N	σ	ϵ	N	σ	ϵ	N	σ	ϵ	N	σ	ϵ	N	σ
$2\pi 2K 1\pi^0$	13.3	3	2.0	14.5	18	6.4	14.1	8	3.4	12.0	0	0.0	13.1	30	8.9	2.6	5	2.1
$3\pi 1K 1K_S^0$	12.3	0	0.0	13.0	11	5.6	12.8	4	2.9	11.0	0	0.0	12.7	10	4.4	12.1	4	2.1
$3\pi 1K 1K_S^0 2\pi^0$	2.8	1	0.0	3.0	6	2.2	3.0	11	3.9	2.8	0	0.0	2.8	15	5.1	2.8	7	2.3
$4\pi 2\pi^0$	8.0	0	0.1	9.0	46	8.5	8.1	19	4.3	7.6	1	0.5	8.0	36	6.7	7.5	23	4.3
$4\pi 2K$	17.8	7	3.5	18.7	18	6.3	18.4	14	4.9	16.2	4	2.4	16.9	12	4.6	16.1	11	4.4
$4\pi 2K 1\pi^0$	8.9	3	1.4	9.8	22	6.2	9.0	13	4.1	8.4	2	1.5	9.2	38	8.9	8.3	16	4.2
$4\pi 2K 2\pi^0$	4.3	3	1.1	4.7	26	6.2	4.3	11	3.2	3.5	7	2.5	3.8	27	6.5	3.9	14	3.7
$5\pi 1K 1K_S^0 1\pi^0$	3.5	0	0.0	3.6	21	6.3	3.9	6	2.4	3.6	4	2.2	3.5	17	5.5	3.5	6	2.2
6π	19.7	2	1.2	21.7	25	7.8	20.6	9	3.6	17.4	1	0.7	19.5	18	5.9	18.1	14	4.7
$6\pi 2\pi^0$	4.3	3	0.8	5.0	56	9.8	5.0	34	6.4	4.5	11	2.5	4.7	44	7.1	4.5	45	6.7
$6\pi 2K$	10.7	9	3.7	12.4	21	6.7	12.1	3	1.3	9.9	2	1.1	10.7	16	5.1	10.6	12	4.2
$6\pi 2K 1\pi^0$	5.1	9	2.9	5.9	28	7.3	5.8	14	4.3	4.6	6	2.9	5.4	25	7.0	4.9	16	5.1
8π	12.7	0	0.4	13.9	24	7.9	12.9	7	3.7	10.7	3	1.8	11.9	16	5.4	11.4	9	3.2
$8\pi 2\pi^0$	2.8	11	2.8	2.9	26	5.5	2.4	29	5.7	2.3	0	0.1	2.6	41	7.5	2.6	27	4.8

Table I shows efficiencies, yields, and signal significances (obtained using the method described earlier) for each of the 14 modes of $\Upsilon(2, 3S) \to \gamma\chi_{bJ}(1P, 2P)$. Table II shows the measured product branching fractions $\mathcal{B}[\Upsilon(nS) \to \gamma\chi_{bJ}((n-1)P)]\mathcal{B}[\chi_{bJ}((n-1)P) \to X_i]$, for $n = 2$ and 3, in units of 10^{-5}. For all transitions with significance less than 3σ, we set upper limits at 90% confidence level (C.L.) in the table. We obtain these limits (Bayesian upper limits with uniform priors) by integrating the likelihood functions. Table III shows the measured values of $\mathcal{B}[\chi_{bJ}((n-1)P) \to X_i]$ obtained using the values of $\mathcal{B}[\Upsilon(nS) \to \gamma\chi_{bJ}((n-1)P)] = (3.8 \pm 0.4, 6.9 \pm 0.4, 7.15 \pm 0.35)\%$ for $n = 2$ and $(5.9 \pm 0.6, 12.6 \pm 1.2, 13.1 \pm 1.6)\%$ for $n = 3$, and for $J = 0$, 1, and 2, respectively [1], whose uncertainties are also included in the systematic errors.

As expected for particles of mass $\sim$10 GeV/c^2, exclusive decays are distributed over many final states. The values of $\mathcal{B}[\chi_{bJ}((n-1)P) \to X_i]$ listed in Table III are typically a few parts in 10^4, suggesting that the decay modes of these 10 GeV particles are distributed over more than a thousand different modes, of which we have investigated 659. Several points are worth noting.

TABLE II. Values of $\mathcal{B}[\Upsilon(nS) \to \gamma\chi_{bJ}((n-1)P)]\mathcal{B}[\chi_{bJ}((n-1)P) \to X_i]$ (10^{-5}). Upper limits at 90% C.L. are set for modes with less than 3σ significance (see Table I).

	$J=0$		$J=1$		$J=2$	
X_i	$n=2$	$n=3$	$n=2$	$n=3$	$n=2$	$n=3$
$2\pi 2K 1\pi^0$	<0.6	<0.2	$1.4 \pm 0.3 \pm 0.3$	$3.9 \pm 0.8 \pm 0.9$	$0.6 \pm 0.3 \pm 0.2$	<1.4
$3\pi 1K 1K_S^0$	<0.2	<0.3	$0.9 \pm 0.3 \pm 0.2$	$1.4 \pm 0.5 \pm 0.3$	<0.7	<1.2
$3\pi 1K 1K_S^0 2\pi^0$	<1.8	<1.3	<4.2	$9.7 \pm 3.0 \pm 2.6$	$3.8 \pm 1.4 \pm 1.0$	<8.7
$4\pi 2\pi^0$	<0.8	<1.4	$5.5 \pm 0.9 \pm 1.4$	$7.4 \pm 1.6 \pm 1.9$	$2.5 \pm 0.8 \pm 0.6$	$5.1 \pm 1.6 \pm 1.3$
$4\pi 2K$	$0.4 \pm 0.2 \pm 0.1$	<0.9	$1.0 \pm 0.3 \pm 0.2$	$1.2 \pm 0.4 \pm 0.3$	$0.8 \pm 0.2 \pm 0.2$	$1.2 \pm 0.4 \pm 0.3$
$4\pi 2K 1\pi^0$	<1.0	<1.3	$2.4 \pm 0.6 \pm 0.6$	$6.9 \pm 1.3 \pm 1.7$	$1.5 \pm 0.5 \pm 0.4$	$3.2 \pm 1.1 \pm 0.8$
$4\pi 2K 2\pi^0$	<2.0	<6.3	$5.9 \pm 1.4 \pm 1.7$	$12.1 \pm 2.9 \pm 3.3$	$2.8 \pm 1.1 \pm 0.7$	$6.2 \pm 2.3 \pm 1.7$
$5\pi 1K 1K_S^0 1\pi^0$	<0.6	<3.9	$6.4 \pm 1.6 \pm 1.6$	$8.5 \pm 2.3 \pm 2.2$	<3.6	<5.8
6π	<0.3	<0.4	$1.3 \pm 0.3 \pm 0.3$	$1.5 \pm 0.4 \pm 0.3$	$0.5 \pm 0.2 \pm 0.1$	$1.2 \pm 0.4 \pm 0.3$
$6\pi 2\pi^0$	<2.2	<7.2	$11.9 \pm 1.8 \pm 3.2$	$15.0 \pm 3.0 \pm 4.0$	$7.3 \pm 1.6 \pm 2.0$	$15.9 \pm 3.3 \pm 4.3$
$6\pi 2K$	$0.9 \pm 0.4 \pm 0.2$	<0.9	$1.8 \pm 0.4 \pm 0.4$	$2.5 \pm 0.7 \pm 0.6$	<0.6	$1.9 \pm 0.7 \pm 0.5$
$6\pi 2K 1\pi^0$	<3.7	<4.3	$5.2 \pm 1.1 \pm 1.4$	$7.7 \pm 1.7 \pm 2.1$	$2.6 \pm 0.8 \pm 0.7$	$5.5 \pm 1.6 \pm 1.5$
8π	<0.3	<1.0	$1.8 \pm 0.4 \pm 0.5$	$2.2 \pm 0.6 \pm 0.5$	$0.6 \pm 0.2 \pm 0.2$	$1.2 \pm 0.5 \pm 0.3$
$8\pi 2\pi^0$	<7.7	<3.8	$9.6 \pm 2.4 \pm 2.9$	$24.1 \pm 4.7 \pm 7.2$	$13.2 \pm 3.1 \pm 4.0$	$16.5 \pm 4.6 \pm 5.0$

TABLE III. Values of $\mathcal{B}[\chi_{bJ}((n-1)P) \to X_i]\,(10^{-4})$. Upper limits at 90% C.L. are set for modes with less than 3σ significance (see Table I).

	$J=0$		$J=1$		$J=2$	
X_i	$n=2$	$n=3$	$n=2$	$n=3$	$n=2$	$n=3$
$2\pi 2K 1\pi^0$	<1.6	<0.3	$2.0 \pm 0.5 \pm 0.5$	$3.0 \pm 0.6 \pm 0.8$	$0.9 \pm 0.4 \pm 0.2$	<1.1
$3\pi 1K 1K_S^0$	<0.5	<0.5	$1.3 \pm 0.4 \pm 0.3$	$1.1 \pm 0.4 \pm 0.3$	<1.2	<0.9
$3\pi 1K 1K_S^0 2\pi^0$	<4.7	<2.3	<6.1	$7.7 \pm 2.3 \pm 2.2$	$5.3 \pm 1.9 \pm 1.5$	<6.7
$4\pi 2\pi^0$	<2.1	<2.5	$7.9 \pm 1.4 \pm 2.1$	$5.9 \pm 1.2 \pm 1.6$	$3.5 \pm 1.1 \pm 0.9$	$3.9 \pm 1.2 \pm 1.1$
$4\pi 2K$	$1.2 \pm 0.5 \pm 0.3$	<1.5	$1.5 \pm 0.4 \pm 0.4$	$0.9 \pm 0.3 \pm 0.2$	$1.2 \pm 0.3 \pm 0.3$	$0.9 \pm 0.3 \pm 0.2$
$4\pi 2K 1\pi^0$	<2.7	<2.2	$3.4 \pm 0.8 \pm 0.9$	$5.5 \pm 1.0 \pm 1.5$	$2.1 \pm 0.7 \pm 0.5$	$2.4 \pm 0.8 \pm 0.7$
$4\pi 2K 2\pi^0$	<5.4	<10.8	$8.6 \pm 2.0 \pm 2.4$	$9.6 \pm 2.3 \pm 2.8$	$3.9 \pm 1.6 \pm 1.1$	$4.7 \pm 1.8 \pm 1.4$
$5\pi 1K 1K_S^0 1\pi^0$	<1.7	<6.7	$9.2 \pm 2.3 \pm 2.5$	$6.7 \pm 1.9 \pm 1.9$	<5.0	<4.5
6π	<0.8	<0.7	$1.8 \pm 0.4 \pm 0.4$	$1.2 \pm 0.3 \pm 0.3$	$0.7 \pm 0.3 \pm 0.2$	$0.9 \pm 0.3 \pm 0.2$
$6\pi 2\pi^0$	<5.9	<12.3	$17.2 \pm 2.7 \pm 4.8$	$11.9 \pm 2.4 \pm 3.4$	$10.2 \pm 2.2 \pm 2.8$	$12.1 \pm 2.5 \pm 3.6$
$6\pi 2K$	$2.4 \pm 0.9 \pm 0.7$	<1.5	$2.6 \pm 0.6 \pm 0.7$	$2.0 \pm 0.6 \pm 0.5$	<0.8	$1.4 \pm 0.5 \pm 0.4$
$6\pi 2K 1\pi^0$	<9.9	<7.3	$7.5 \pm 1.6 \pm 2.1$	$6.1 \pm 1.4 \pm 1.8$	$3.7 \pm 1.2 \pm 1.0$	$4.2 \pm 1.2 \pm 1.2$
8π	<0.7	<1.7	$2.7 \pm 0.6 \pm 0.7$	$1.7 \pm 0.5 \pm 0.5$	$0.8 \pm 0.4 \pm 0.2$	$0.9 \pm 0.4 \pm 0.3$
$8\pi 2\pi^0$	<20.5	<6.5	$14.0 \pm 3.5 \pm 4.3$	$19.2 \pm 3.7 \pm 6.0$	$18.5 \pm 4.4 \pm 5.6$	$12.6 \pm 3.5 \pm 4.1$

(1) The mode with the largest branching ratio which we have identified is $6\pi 2\pi^0$. Its branching ratios from the $\chi_{b1,2}(1P, 2P)$ states are approximately an order of magnitude larger than those for the 6π mode. Modes with charged pions and an odd number of neutral pions are forbidden by G-parity unless subsystems contain isospin-violating decays such as $\eta \to \pi^+\pi^-\pi^0$. Indeed, $6\pi\pi^0$ and $6\pi 3\pi^0$ decays are not seen at a statistically significant level. The $6\pi 4\pi^0$ mode involves 14 particles, while we consider modes with a maximum of 12.

(2) The branching ratios for $8\pi 2\pi^0$ states from $\chi_{b1,2}(1P, 2P)$ also exceed those for 8π by a considerable margin. Again, G-parity conservation explains why one does not see a significant signal for $8\pi\pi^0$.

(3) Modes with one or more $K\bar{K}$ pairs in addition to charged pions are exempt from the G-parity selection rule because a $K\bar{K}$ pair can have either G-parity.

(4) The $4\pi 2\pi^0$ mode has a larger significance than either 4π or $4\pi 4\pi^0$. Typically in the decay of an isospin-zero particle, one should expect to see the same number of π^+, π^-, and π^0 [10], and this is reflected to some extent in individual modes.

(5) The 14 modes constitute a total of less than a percent of all expected hadronic modes of the $\chi_{b1,2}(1P)$ states. The ability to identify even such a small subset of the $\chi_{b1}(1P, 2P)$ hadronic decays depends to a large extent on CLEO's ability to reconstruct one or more neutral pions. Using only charged tracks, one would reconstruct an order of magnitude fewer decays.

We have also studied the E1 transitions $\Upsilon(3S) \to \gamma\chi_{bJ}(1P)$. These transitions are suppressed by small overlaps of wave functions in the dipole matrix element $\langle 1P|\vec{r}|3S\rangle$ [11]. We investigate the ratios

$$R_J \equiv \frac{\mathcal{B}[\Upsilon(3S) \to \gamma\chi_{bJ}(1P)]}{\mathcal{B}[\Upsilon(2S) \to \gamma\chi_{bJ}(1P)]}, \qquad (1)$$

where the ratios of branching fractions are determined from fitted yields in $\Upsilon(3S)$ and $\Upsilon(2S)$ data, respectively, corrected for small differences in signal efficiencies. In modes with any neutral pions or η mesons, substantial backgrounds arise from subsequent $\chi_{bJ}(1P) \to \gamma\Upsilon(1S)$ decays, whose photons are similar in energy to those in

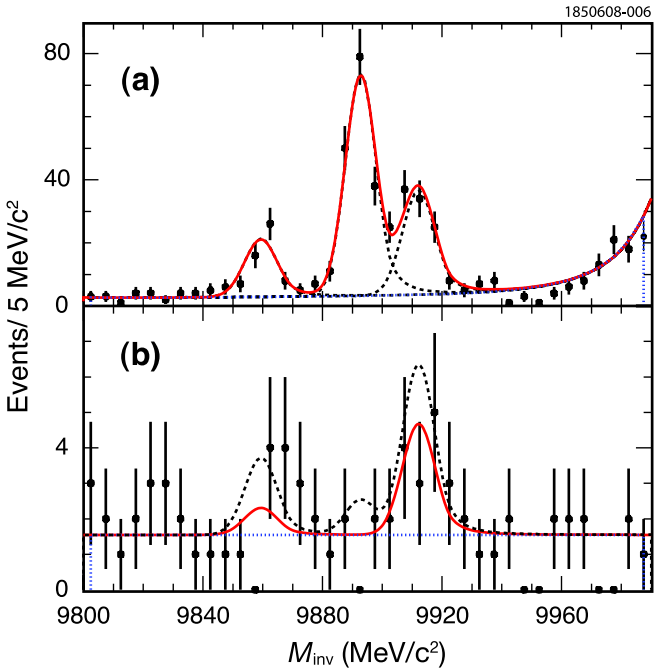

FIG. 3 (color online). Comparison of spectra, based on 167 modes not involving π^0 or η mesons, in transitions from (a) $\Upsilon(2S) \to \gamma\chi_b(1P)$ and (b) $\Upsilon(3S) \to \gamma\chi_b(1P)$. The background shape in (a) is derived from $\Upsilon(1S)$ data as described in the text. The dashed lines in (a) are fitted $\chi_{bJ}(nP)$ signals of each J state while those in (b) correspond to 90% C.L. upper limits on signal yields.

$\Upsilon(3S) \to \gamma\chi_{bJ}(1P)$. To eliminate such backgrounds, we restrict attention to 167 modes not involving π^0 or η mesons. Figure 3(a) shows the $M_{\rm inv}$ distribution based on the sum of such modes in $\Upsilon(2S)$ data. The background is represented by the exponential of a polynomial, fitted to a *shifted* invariant mass distribution of $\Upsilon(1S)$ data (smooth dotted curve), and the peak positions are fixed at the known masses [1]. Using the $\chi_{bJ}(1P)$ signal shapes obtained in this fit, we fit $\Upsilon(3S)$ data with a constant background, as shown in Fig. 3(b). The fit gives statistical significances of 0.7σ, 0.0σ, and 2.6σ for signals consistent with the transitions $\Upsilon(3S) \to \gamma\chi_{b0,1,2}(1P)$, respectively. We find $R_2 = (15.7 \pm 7.6 \pm 2.2) \times 10^{-2}$ and 90% C.L. upper limits $R_{(0,1,2)} < (21.9, 2.5, 27.1) \times 10^{-2}$. Using known values of $\mathcal{B}[\Upsilon(2S) \to \gamma\chi_b(1P)]$ [1], we then find $\mathcal{B}[\Upsilon(3S) \to \gamma\chi_{b2}(1P)] = [11 \pm 6(\text{stat}) \pm 2(\text{syst}) \pm 1] \times 10^{-3}$, where the last uncertainty comes from $\mathcal{B}[\Upsilon(2S) \to \gamma\chi_{b2}(1P)]$ [1]. While most systematic uncertainties are canceled in the ratio of yields, our total uncertainty (14%) is dominated by variations in the signal as we change the width of the range over which we fit $\Upsilon(3S)$ decays. Our nominal fit range is 9800–9990 MeV, varied to 9800–9950 MeV and 9750–10050 MeV. Although this variation is well within statistical fluctuations, we conservatively take it as a possible systematic uncertainty.

We set 90% C.L. upper limits $\mathcal{B}[\Upsilon(3S) \to \gamma\chi_{b0}(1P)] < 9.2 \times 10^{-3}$, consistent with the value of $(3.0 \pm 0.4 \pm 1.0) \times 10^{-3}$ reported in Ref. [4], $\mathcal{B}[\Upsilon(3S) \to \gamma\chi_{b1}(1P)] < 1.9 \times 10^{-3}$, and $\mathcal{B}[\Upsilon(3S) \to \gamma\chi_{b2}(1P)] < 20.3 \times 10^{-3}$. Our results are compared with some theoretical predictions in Table IV.

TABLE IV. Comparison of measurements and predictions [12] for suppressed E1 transition rates in units of eV. Experimental measurements are based on $\Gamma_{\Upsilon(3S)} = 20.32$ keV [1].

	$J=0$	$J=1$	$J=2$
Inclusive experiment [4]	61 ± 22	...	...
Exclusive experiment (this work)	<186	<38	<413
Moxhay–Rosner (1983)	25	25	150
Grotch *et al.* (1984)[a]	114	3.4	194
Grotch *et al.* (1984)[b]	130	0.3	430
Daghighian–Silverman (1987)	16	100	650
Fulcher (1990)	10	20	30
Lähde (2003)	150	110	40
Ebert *et al.* (2003)	27	67	97

[a]Confining potential is purely scalar.
[b]Confining potential is purely vector.

We have presented the first observations of decays of $\chi_{bJ}(1P)$ and $\chi_{bJ}(2P)$ to exclusive final states of light hadrons. These results can be of use in validating models for fragmentation of heavy states, and in searching for states of mass $\sim 10\ \text{GeV}/c^2$ via their exclusive decays. We also find upper limits for the rates of the suppressed E1 transitions $\Upsilon(3S) \to \gamma\chi_{b0,1,2}(1P)$.

We gratefully acknowledge the effort of the CESR staff in providing us with excellent luminosity and running conditions. D. Cronin-Hennessy and A. Ryd thank the A.P. Sloan Foundation. This work was supported by the National Science Foundation, the U.S. Department of Energy, the Natural Sciences and Engineering Research Council of Canada, and the U.K. Science and Technology Facilities Council.

[1] C. Amsler *et al.* (Particle Data Group), Phys. Lett. B **667**, 1 (2008).
[2] R. A. Briere *et al.* (CLEO Collaboration), Phys. Rev. D **76**, 012005 (2007).
[3] R. A. Briere *et al.* (CLEO Collaboration), arXiv:0807.3757 [Phys. Rev. D (to be published)].
[4] M. Artuso *et al.* (CLEO Collaboration), Phys. Rev. Lett. **94**, 032001 (2005).
[5] Y. Kubota *et al.* (CLEO Collaboration), Nucl. Instrum. Methods Phys. Res., Sect. A **320**, 66 (1992); D. Peterson *et al.* (CLEO Collaboration), Nucl. Instrum. Methods Phys. Res., Sect. A **478**, 142 (2002); M. Artuso *et al.* (CLEO Collaboration), Nucl. Instrum. Methods Phys. Res., Sect. A **502**, 91 (2003).
[6] R. E. Mitchell *et al.* (CLEO Collaboration), arXiv:0805.0252 [Phys. Rev. Lett. (to be published)].
[7] W. Kwong and J. L. Rosner, Phys. Rev. D **38**, 279 (1988).
[8] J. E. Gaiser, Ph.D. thesis, Stanford Univ., Stanford, CA [Report No. SLAC-R-255, 1982 (unpublished)]; T. Skwarnicki, Ph.D. thesis, Cracow Inst. of Nucl. Phys., Cracow [Report No. DESY-F31-86-02, 1986 (unpublished)].
[9] R. Brun *et al.*, GEANT 3.21, CERN Program Library Long Writeup W5013, 1993 (unpublished).
[10] E. Fermi, Phys. Rev. **92**, 452 (1953); **93**, 1434(E) (1954); K. M. Watson, Phys. Rev. **85**, 852 (1952); I. Smushkevich, Dokl. Akad. Nauk SSSR **103**, 235 (1955); A. Pais, Ann. Phys. (N.Y.) **9**, 548 (1960); **22**, 274 (1963); M. Peshkin, Phys. Rev. **121**, 636 (1961); M. Peshkin and J. L. Rosner, Nucl. Phys. **B122**, 144 (1977).
[11] A. K. Grant and J. L. Rosner, Phys. Rev. D **46**, 3862 (1992).
[12] P. Moxhay and J. L. Rosner, Phys. Rev. D **28**, 1132 (1983); S. N. Gupta, S. F. Radford, and W. W. Repko, Phys. Rev. D **30**, 2424 (1984); H. Grotch, D. A. Owen, and K. J. Sebastian, Phys. Rev. D **30**, 1924 (1984); F. Daghighian and D. Silverman, Phys. Rev. D **36**, 3401 (1987); J. P. Fulcher, Phys. Rev. D **42**, 2337 (1990); T. A. Lähde, Nucl. Phys. **A714**, 183 (2003); D. Ebert, R. N. Faustov, and V. O. Galkin, Phys. Rev. D **67**, 014027 (2003).